Transactions of the **14th International Conference on Structural Mechanics in Reactor Technology** (SMiRT 14), Lyon, France, August 17-22, 1997 **K05/2**

Simulation analyses of a reactor building's responses in the 1995 Great Hanshin earthquake

Kowada A.(1), Kitano T.(1), Akita S.(1), Kosaka K.(1), Ohori M.(2), Tanaka H.(2)
(1) The Kansai Electric Power Co., Inc., Japan
(2) Obayashi Corporation, Japan

ABSTRACT: This paper describes simulation analyses of earthquake records of the 1995 Great Hanshin Earthquake at a nuclear reactor building of the Ohi Nuclear Power Station of The Kansai Electric Power Co., Inc. Simulation analyses based on a lumped mass model were done for horizontal responses and vertical ones. Also, a detailed model was used to reproduce horizontal responses. Through the study, it was concluded from an engineering point of view that the lumped mass model is sufficient for the aseismic design.

1. INTRODUCTION

The Unit No.3 and the Unit No.4 of the Ohi Nuclear Power Station (ONPS) are PWR (Pressurized Water Reactor) type 4-loop reactors, each of which has 1,180MW electric capacity. Two buildings are identically designed and vibration characteristics of them are expected to be identical. Earthquake observations have been done in those two reactor buildings, but mainly in Unit No.4 of our interest and auxiliary in No.3. Then during the 1995 Great Hanshin Earthquake (the Hyogo-Ken Nanbu Earthquake) of January 17, precious accelerograms were recorded at the plant. As it was the closest nuclear power station from the epicenter of the earthquake, the observed accelerograms deserve to be reported. In this paper, we therefore describe the characteristics of the acceleration records observed at the plant and simulation analysis results of the records both for horizontal responses and for vertical responses.

2. EARTHQUAKE OBSERVATION AND RECORDS

2.1 THE 1995 HYOGO-KEN NANBU EARTHQUAKE

On January 17, 1995, a 7.2 magnitude earthquake hit the southern Hyogo Prefecture and took about 6,300 persons' lives and demolished about one hundred thousand residential houses. It consequently resulted in the second worst earthquake disaster in Japan after the 1923 Great Kanto Earthquake. This earthquake occurred at the north of Awajishima Island and its rupture on the fault plane propagated to Kobe and to the south of Awajishima Island. Japan Meteorological Agency (JMA) marked the JMA seismic intensity scale of 7 at the most devastated area in Kobe, its surroundings, and the northern Awajishima. Kobe Marline Station of JMA observed the maximum horizontal acceleration of 818 gal. On the other hand, the reactor building was standing on the stiff bedrock, about 120 km north-northeast from the

epicenter as shown in Fig.1. It had no damage in all facilities and functions. It was the closest reactor building from the epicenter of the earthquake. By the way, at Maizuru Marline Station of JMA, very close to this plant, the maximum acceleration of 67 gal was observed on the soft ground. This is about five times larger than the maximum acceleration of the ground motion at the plant as mentioned later. It is clear that the ground motion is not amplified so much at the site on stiff rock.

2.2 EARTHQUAKE RECORDS

Earthquake observations have been done mainly in the Unit No.4 and auxiliary in No.3, and during the earthquake, accelerograms were observed. In Fig.2, a cross section of the building is shown. The reactor building consists of the inner concrete structure (I/C), the prestressed concrete containment vessel (PCCV), and the external building (E/B), which are standing on the same basemat (B/M) with thickness of 11.1 m. Also the location of sensors installed in the Unit No.4 is shown in Fig.2 with the black solid circles. The I/C and the PCCV are of our interest. Observed accelerograms and those Fourier spectra are shown in Fig.3 through Fig.5. As remarkable differences were not found between the seismic characteristics of NS component and those of EW component, NS and UD components were shown in Fig.3 and Fig.4. With respect to UD component of the I/C, the machinery noise around the sensor was at the high level and it made the S/N ratio small during the earthquake. Therefore our attention was paid to NS and EW components in Fig.5. The maximum accelerations in horizontal components are 12.7 gal at below the bottom of the B/M, 108.3 gal at the top of the PCCV, and 25.0 gal at the operating floor of the I/C. Those in vertical components are 11.7 gal at below the bottom of the B/M, 20.7 gal at the top of the PCCV.

3. SIMULATION ANALYSES OF HORIZONTAL RESPONSES

3.1 SIMULATION MODEL

Preceding earthquake observations, forced vibration tests were carried out for the reactor building of the Unit No.3 to obtain vibration characteristics of horizontal direction, such as natural frequencies and damping factors of the I/C and the PCCV. Detailed description about test results is found in ref.[1]. The resonance curves obtained from tests were simulated well with a lumped mass model in Fig.6(a) and simulated better with more detailed model in Fig.6(b). The vibration characteristics of the reactor building of the Unit No.3 is considered to be identical with those of the Unit No.4. Also, the strain levels induced by the earthquake were not so large compared with those in vibration tests. We therefore used the same models for earthquake responses analyses. The lumped mass model in Fig.6(a) was a design-based model. The detailed model in Fig.6(b) was the same as the lumped mass model except for the I/C replaced by FEM. We refer to this model as the I/C FEM model hereafter. As for material properties, the Young's modulus of the concrete was set to 3.9×10^5 kgf/cm^2 for the PCCV and to 3.4×10^5 kgf/cm^2 for the others. And the damping factors was set to 2 % for the PCCV and to 3 % for the others. To take into account the dynamic interaction between the soil and the foundation, the frequency dependent complex stiffness based on the wave propagation theory was evaluated and used in simulation analyses. In simulation analyses, observed accelerograms at below the bottom of the B/M were used as input motions.

3.2 SIMULATION OF PCCV

Accelerograms and those Fourier spectra from simulation analyses calculated with the lumped mass model are compared with those from earthquake records in Fig.7 and Fig.8. From these figures, it was found that analyzed results for the PCCV were in good agreement with observed ones for both NS and EW components. The maximum acceleration values of records and analyses are compared in Table 1. Also, a good agreement was found in spectral ratio of

the PCCV to the input motion for each horizontal direction although it was not shown because of the limited space. Moreover, the peak frequency of the spectral ratio was 5.0 Hz, which was equal to the natural frequency of the PCCV obtained from forced vibration tests.

Table 1 The Maximum Acceleration of the PCCV of Horizontal Responses

Structure	Direction	Analyses	Records	Analyses / Records
PCCV	NS	96.9 gal	84.7 gal	1.14
	EW	105.0 gal	108.3 gal	0.97

3.3 SIMULATION OF I/C

Accelerograms and those Fourier spectra from simulation analyses using the lumped mass model are compared with those from earthquake records in Fig.9 and Fig.10. Also, accelerograms and those Fourier spectra from simulation analyses with the I/C FEM model are compared with those from earthquake records in Fig.11 and Fig.12. From Fig.9 and Fig.10, differences between results of analyses and those of observations are not significant when the lumped mass model was used. But we can confirmed from Fig.11 and Fig.12 that these differences are improved with use of the I/C FEM model. Especially, in the frequency range around 10 Hz of the NS component, the I/C FEM model reproduces successfully observed responses as shown in Fig.11, whereas the lumped mass model fails to do it. Relatively, as for the EW component, both two models express well observed responses. The maximum acccceleration values of records and analyses are compared in Table 2. It depends on acceptance level of simulation results whether more detailed model would be required or not. But judging from an engineering point of view, the lumped mass model is sufficient for the aseismic design. Also, earthquake records were simulated well with use of two models in Fig.6(a) and Fig.6(b) which were made for the simulation of forced vibration tests. It follows that forced vibration tests are useful to construct the earthquake simulation model.

Table 2 The Maximum Acceleration of the I/C Horizontal Responses.

Structure	Direction	Model	Analyses	Records	Analyses / Records
I/C	NS	Lumped Mass	22.6 gal	18.0 gal	1.26
		I/C FEM	20.9 gal	18.0 gal	1.16
	EW	Lumped Mass	24.7 gal	25.0 gal	0.99
		I/C FEM	25.6 gal	25.0 gal	1.02

4. SIMULATION ANALYSES OF VERTICAL RESPONSES

4.1 SIMULATION MODEL

The lumped mass model in Fig.6(c) was used for simulation analyses of vertical responses. This model was almost the same as the one in Fig.6(a) except for the following points. First, to express the vibration of the PCCV's dome accurately, two nodes were newly added there. Second, the weight of the Steam Generator (S/G) were included to the corresponding nodes of the I/C because interactive behavior between the I/C and S/G was negligible in vertical responses. Third, after the frequency dependent complex stiffness was obtained from the

wave propagation theory, it was simplified into the system of equivalent spring and viscous damper taking into account the 1st natural frequency of the whole building obtained from the eigenvalue problem analysis.

4.2 SIMULATION OF PCCV

Accelerograms and those Fourier spectra from simulation analyses calculated with the lumped mass model are compared with those from earthquake records in Fig.13 and Fig.14. From these figures, it was found that analyzed results for the PCCV were in good agreement with observed ones both for the top of the dome and for the top of the cylinder. The maximum accceleration values of records and analyses are compared in Table 3. Focusing on the ratio of the observed maximum acceleration between the top of the PCCV to the gound motion, it was about 1.8 in vertical responses, whereas it was about 6.7 in NS and 9.9 in EW. The amplification of PCCV in vertical responses was small compared with horizontal responses.

Table 3 The Maximum Acceleration of the PCCV Vertical Responses.

Structure	Location	Analyses	Records	Analyses / Records
PCCV	Top of Dome	24.7 gal	20.7 gal	1.19
	Top of Cylinder	17.1 gal	18.8 gal	0.91

5. CONCLUSIONS

Through this study, the following conclusions are obtained:

1) The vibration characteristics of the I/C and PCCV observed from earthquake records coincided with those from forced vibration tests.
2) Earthquake responses of the PCCV were simulated satisfactorily with use of the lumped mass model both for horizontal responses and for vertical ones. Also, earthquake responses of the I/C were simulated well with use of lumped mass model.
3) From an engineering point of view, the lumped mass model is sufficient for the aseismic design. More detailed model would be required depending on acceptance level of simulation results.
4) The amplification of the maximum acceleration for PCCV was small in vertical responses compared with horizontal responses.

REFERENCES

[1] Setogawa, S., et al., Forced vibration tests on the reactor building of a PWR type nuclear power station, SMiRT-12, K12, 1993, pp.325-330 .

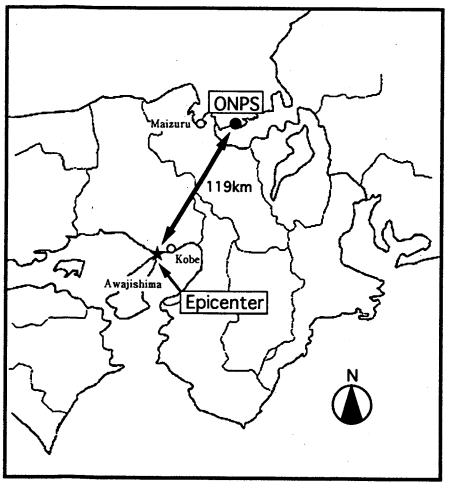

Fig.1 Location map of the epicenter of the 1995 Great Hanshin Earthquake and the Ohi Nuclear Power Station (ONPS).

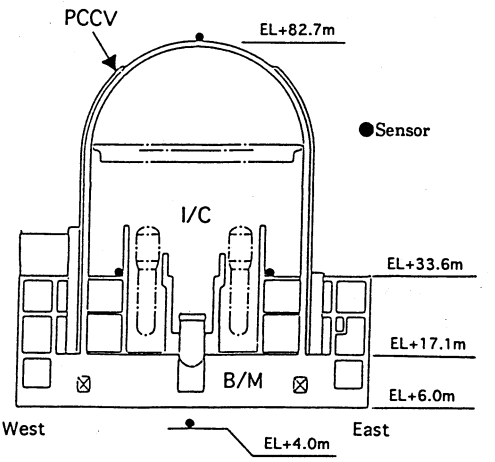

Fig.2 EW section of the reactor building and measuring points in forced vibration tests.

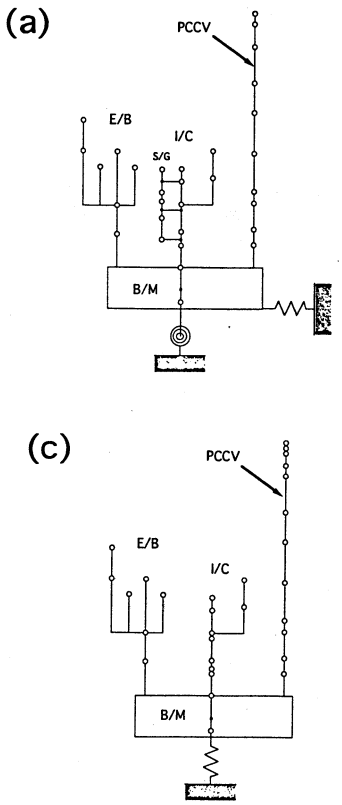

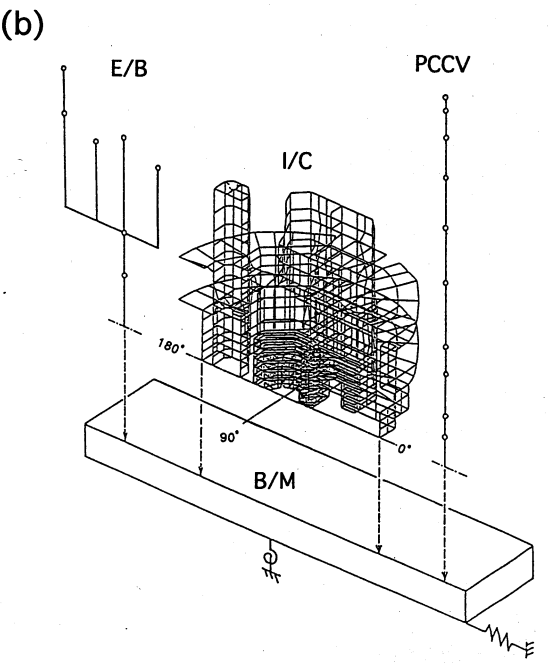

Fig.6 Simulation model.
(a) The lumped mass model for horizonal responses.
(b) The I/C FEM model for horizonal responses.
(c) The lumped mass model for vertical responses.

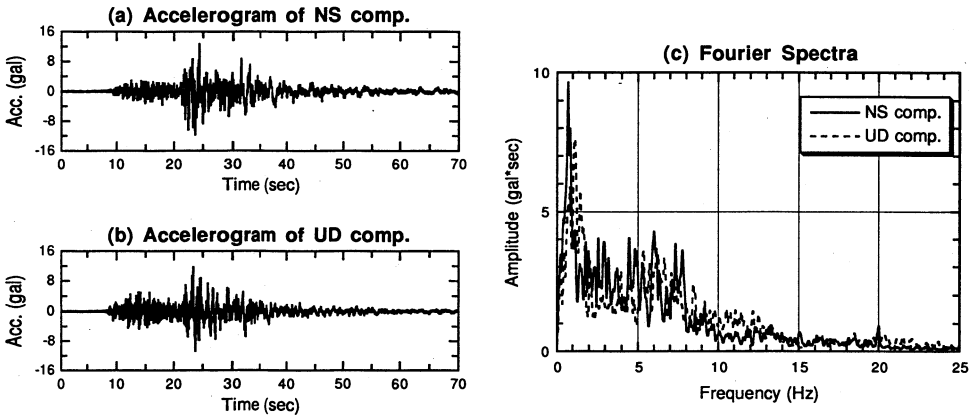

Fig.3 Observed records of the NS and UD components at below the bottom of B/M (EL+4.0m).

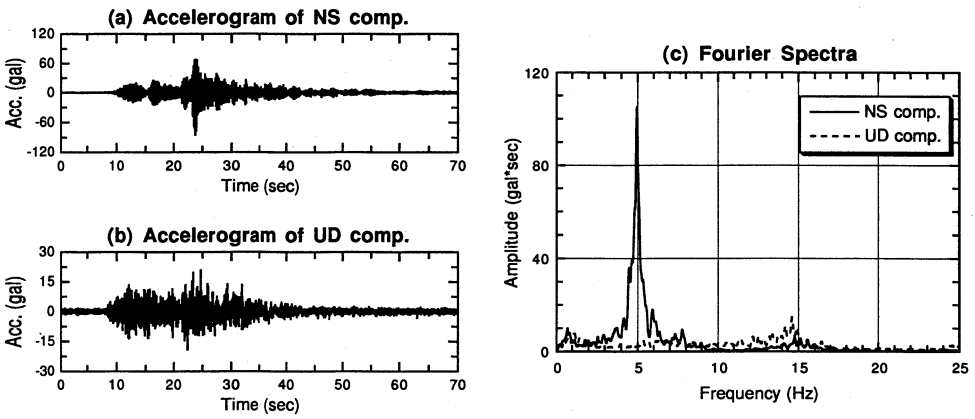

Fig.4 Observed records of the NS and UD components at the top of PCCV (EL+82.7m).

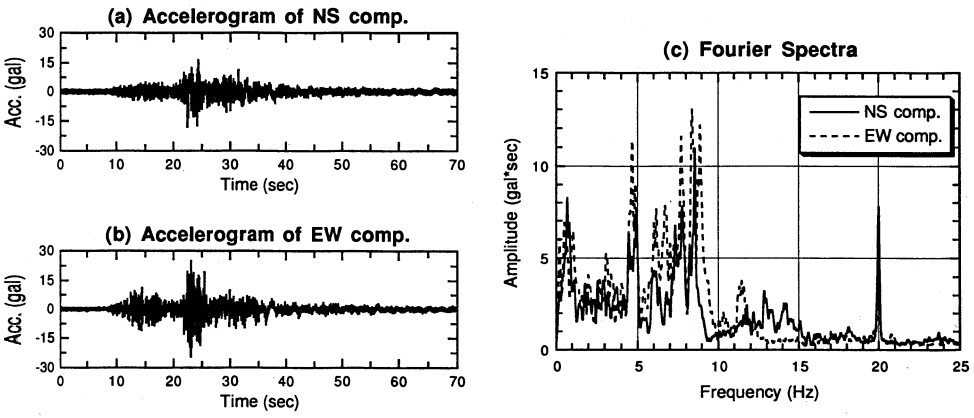

Fig.5 Observed records of the NS and EW components at the operating floor of I/C (EL+33.6m).

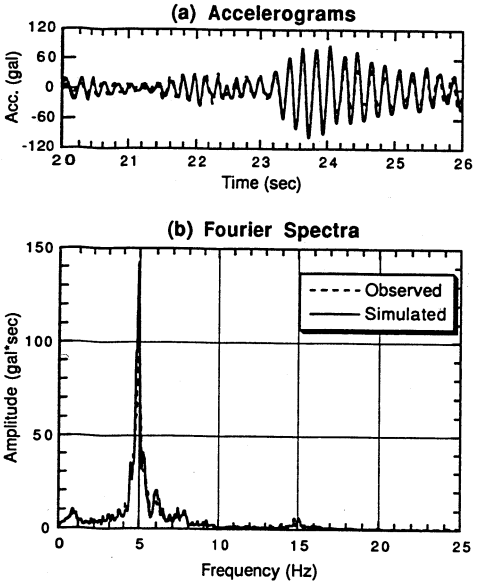

Fig.7 Observed and simulated results of the NS component at the top of PCCV (EL+82.7m). The lumped mass model are used in simulation analyses.

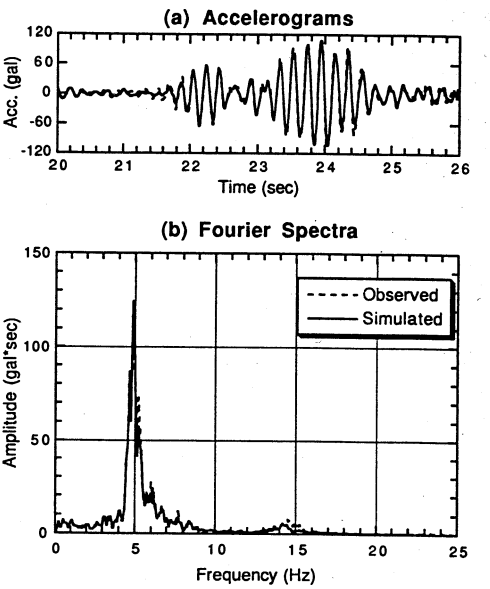

Fig.8 Observed and simulated results of the EW component at the top of PCCV (EL+82.7m). The lumped mass model are used in simulation analyses.

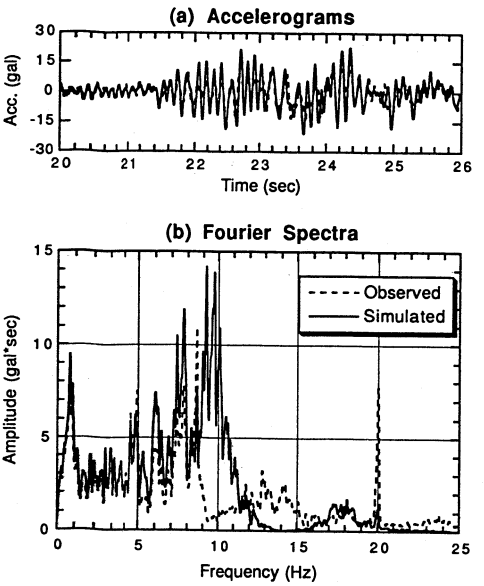

Fig.9 Observed and simulated results of the NS component at the operating floor of I/C (EL+33.6m). The lumped mass model are used in simulation analyses.

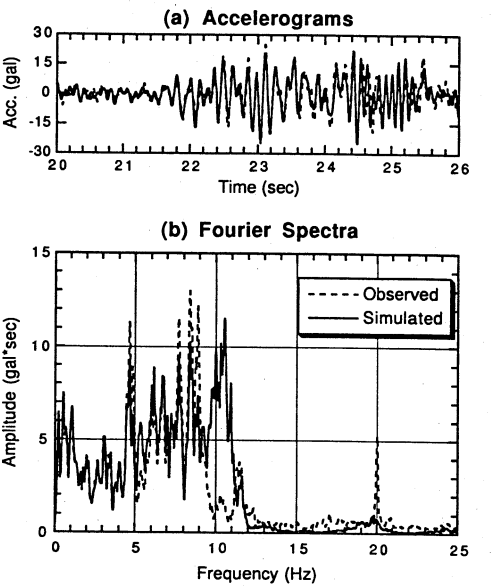

Fig.10 Observed and simulated results of the EW component at the operating floor of I/C (EL+33.6m). The lumped mass model are used in simulation analyses.

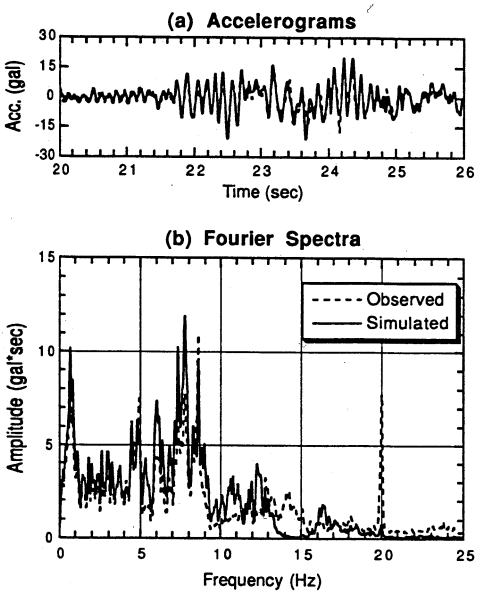

Fig.11 Observed and simulated results of the NS component at the operating floor of I/C (EL+33.6m). The I/C FEM model are used in simulation analyses.

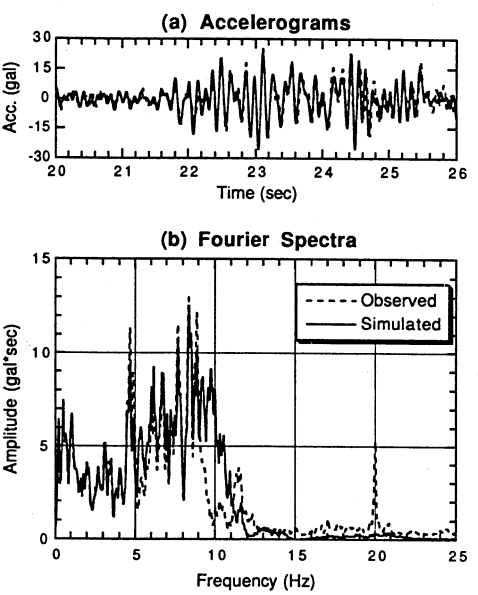

Fig.12 Observed and simulated results of the EW component at the operating floor of I/C (EL+33.6m). The I/C FEM model are used in simulation analyses.

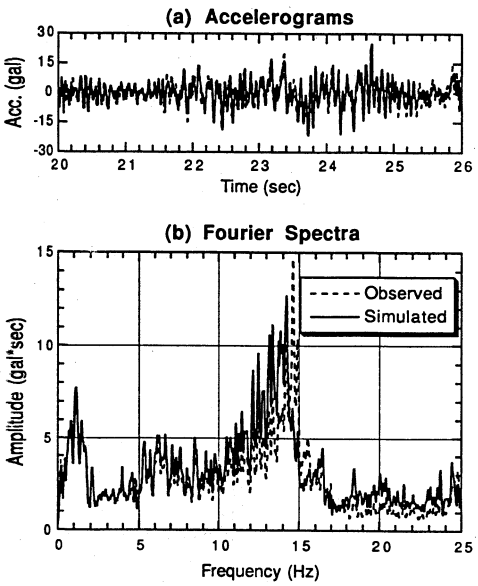

Fig.13 Observed and simulated results of the UD component at the top of PCCV (EL+82.7m). The lumped mass model are used in simulation analyses.

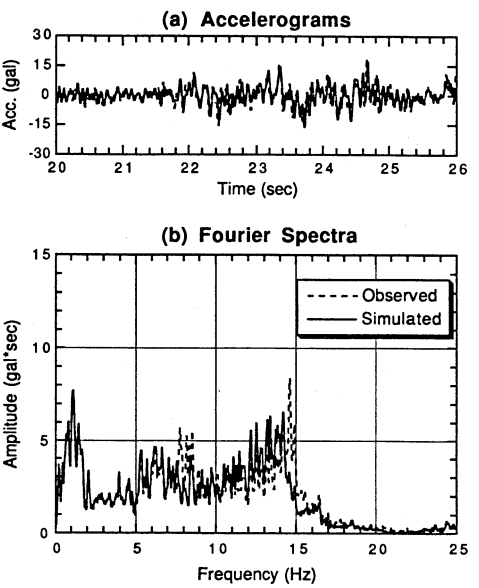

Fig.14 Observed and simulated results of the UD component at the top of PCCV 's cylinder (EL+59.8m). The lumped mass model are used in simulation analyses.